

# Purcell factor enhanced scattering efficiency in optical microcavities

T.J. Kippenberg<sup>1</sup>, A.L. Tchebotareva<sup>2</sup>, J. Kalkman<sup>2</sup>, A. Polman<sup>2</sup>, K.J. Vahala<sup>1\*</sup>

<sup>1</sup> *Thomas J. Watson Laboratory of Applied Physics,  
California Institute of Technology, Pasadena, CA 91125. and*

<sup>2</sup> *Center for Nanophotonics, FOM Institute AMOLF,  
Kruislaan 407, 1098SJ, Amsterdam, The Netherlands.*

## Abstract

Scattering processes in an optical microcavity are investigated for the case of silicon nanocrystals embedded in an ultra-high Q toroid microcavity. Using a novel measurement technique based on the observable mode-splitting, we demonstrate that light scattering is highly preferential: more than 99.8% of the scattered photon flux is scattered into the original doubly-degenerate cavity modes. The large capture efficiency is attributed to an increased scattering rate into the cavity mode, due to the enhancement of the optical density of states over the free space value and has the same origin as the Purcell effect in spontaneous emission. The experimentally determined Purcell factor amounts to 883.

PACS numbers: 42.65Yj, 42.55-Sa, 42.65-Hw

---

\*Electronic address: polman@amolf.nl,vahala@its.caltech.edu,

Optical microcavities confine light both temporally and spatially and find application in a variety of applied and fundamental studies, such as photonics, cavity quantum electrodynamics, nonlinear optics and sensing[1]. In nearly all embodiments of microcavities, such as microdisks, microspheres, micropillars or photonic crystals, sub-wavelength defect centers are present, either caused by intrinsic material irregularities, fabrication imperfection or intentionally induced (such as quantum dots). The concomitant refractive index perturbations lead to scattering, which increases the cavity loss rate. In this manuscript we analyze the effect of scattering in an optical microcavity, using a toroid microcavity containing silicon nanocrystals (Si NCs) as scattering centers. Using a novel measurement technique we demonstrate for that light scattering is highly preferential; 99.8% of all scattered light is scattered into the original eigenmodes. This value cannot be explained by the existing geometrical optics theory[2]. A novel theoretical analysis shows that the observed enhanced scattering rate into the original cavity mode is due to the enhancement of the optical density of states (DOS) over the free space value, and therefore has the same origin as the Purcell-effect in spontaneous emission. The presented experimental and theoretical results establish the significance of the Purcell-factor for scattering processes within a microcavity and constitute the highest experimentally measured Purcell factor to date (883).

It is a well known phenomenon [2, 3, 4] that the resonances of whispering gallery mode (WGM) microcavities such as droplets, microspheres, microtoroids or microdisks appear as doublets. The doublet splitting is due to lifting of the two-fold degeneracy of the clockwise (CW) and counter-clockwise (CCW) whispering-gallery-modes (WGMs) that occurs when these modes are coupled due to scattering, either by intrinsic or surface inhomogeneities. In the Rayleigh limit (particle radius  $r \ll \lambda$ ), this leads a scattered power  $P$  per unit solid angle  $\Omega$  as given by  $\frac{dP}{d\Omega} = \frac{1}{4\pi\epsilon} k^4 |\vec{p}|^2 \cos^2(\theta)$ , with  $\epsilon$  the dielectric constant of the medium,  $k$  the magnitude of the wave vector, and  $\theta$  the scattering angle. As discussed in reference [2] this leads to doublet splitting due to lifting of the CW and CCW mode degeneracy, since part of the scattered light is channeled back into the original pair of eigenmodes, leading to an observable mode splitting. In what follows, it is analyzed how the observable mode splitting can be used to infer the capture efficiency ( $\eta$ ), which is defined as the fraction of light scattered into the original eigenmodes (and which, therefore, does not contribute to cavity losses). For a single nanoparticle scattering cross section  $\sigma_{scat}$ , and a number density  $N$ , the total scattering rate is given by  $\gamma_{tot}^{-1} = \sigma_{scat} N \frac{c}{n}$  where  $c$  is the speed of light. The

mode splitting (in the frequency domain) is then given by

$$\gamma^{-1} = \frac{1}{2}\eta\gamma_{tot}^{-1} \quad (1)$$

The factor of  $\frac{1}{2}$  takes into account that the scattering of light into original eigenmodes (i.e., self-coupling) does not contribute to the observed mode splitting. Owing to the small size of the scattering centers in comparison to the wavelength of light, it is assumed that scattering is equally divided into CW and CCW direction. The dissipation rate of light not scattered into the cavity mode is given by:

$$\tau^{-1} = (1 - \eta)\gamma_{tot}^{-1} \quad (2)$$

In addition,  $1/\tau_0$  will describe losses associated with absorption, and the cumulative effect of these processes ( $1/\tau_0 + 1/\tau$ ) causes a reduction in cavity  $Q$ . The degree to which the scattering process couples the initially degenerate cavity modes can be described by the modal coupling parameter  $\Gamma$  [4], which can be expressed by:

$$\Gamma = \left( \frac{\frac{1}{2}\eta\gamma_{tot}^{-1}}{\tau_0^{-1} + (1 - \eta)\gamma_{tot}^{-1}} \right) \quad (3)$$

$\Gamma$  thus reflects the relative “visibility” of the doublet as appearing in the under-coupled resonance spectrum; measurement of this parameter is described in detail in refs. [3, 4].

The capture efficiency  $\eta$  can be retrieved from  $\Gamma$  as follows. In the presence of other loss channels, such as residual material absorption, two limits of Eq. 3 can be considered. First, if the cavity losses are dominated by absorption, i.e.  $\tau_0^{-1} \gg (1 - \eta)\gamma_{tot}^{-1}$ , Eq. 3 simplifies to:

$$\Gamma = \frac{\eta\gamma_{tot}^{-1}}{2\tau_0^{-1}} \quad (4)$$

i.e. the doublet visibility, measured for different cavity modes, increases linearly with intrinsic  $Q$  (if scattering is constant for all modes). In this regime, a *lower bound* of the capture efficiency  $\eta$  can be found, given by  $\eta > \frac{2\gamma_{tot}\Gamma}{\tau_0}$ . Second, in the scattering-limited case, for which  $\tau_0^{-1} \ll (1 - \eta)\gamma_{tot}^{-1}$  it follows from Eq. 3 that:

$$\eta = \frac{2\Gamma}{1 + 2\Gamma} \quad (5)$$

In this regime an improved *lower bound* of the capture efficiency  $\eta$  can be inferred from measurements of  $\Gamma$  (with the accuracy given by the amount residual absorption). Significantly, in the case where the residual absorption (i.e.  $\tau_0$ ) is known and is identical for all

cavity modes (i.e. an intrinsic property of the resonator)  $\eta$  can be inferred exactly. It can then be determined by measuring  $\Gamma$  for modes with various amounts of scattering ( $\gamma_{tot}$ ), and inferring  $\eta$  via the functional relation of  $\Gamma(Q, \gamma_{tot})$  as given by Eq. 3.

To test the above model, we have investigated the scattering processes of SiO<sub>2</sub> toroid microcavities. These microcavities exhibit ultra-high-Q whispering-gallery type modes [5], and can be used as ultralow threshold chip based Raman lasers, optical parametric oscillators, or erbium microlasers. Details on fabrication and on the coupling technique (using tapered optical fibers) can be found in Refs.[5, 6]

Figure 1 shows measurement of the  $\Gamma$ -parameter for an undoped SiO<sub>2</sub> 50- $\mu$ m-diameter toroid microcavity, measured for successive fundamental resonances with different Q in the 1550 nm band. A cavity resonance scan is shown in the upper right panel of Fig. 1, and shows the typical doublet splitting of  $\sim 10$  MHz observed for pure SiO<sub>2</sub> toroids. The data in the main panel of Fig. 1 clearly follow a linear relationship, indicating that the cavity resonances follow absorption-limited behavior (attributed to adsorbed water and OH on the surface of the toroid[7]). The scattering rate  $\gamma^{-1}/2\pi$  derived from the data is plotted in the lower right figure (as  $Q_{split} = \omega\gamma$ ), and is indeed to a very good approximation the same for all modes. From the highest observed doublet splitting ( $\Gamma = 28$ ) the lower estimate of the capture efficiency is  $\eta > 96.4\%$ . This value cannot be explained by the quasi-geometrical estimations of Ref. [2] which predict a *maximum* capture efficiency of 90%. This model assumes that scattered light obeys a Rayleigh-type angular distribution, and can couple back into the CW and CCW modes, provided the scattering angle  $\theta$  is within the critical angle  $\phi$  of the mode i.e.  $\theta < \phi$ . This model, while adequate to describe losses of a waveguide-bend, is (as will be shown below), incomplete as it neglects the periodic nature of light scattering in a microcavity.

To infer the capture efficiency more exactly, measurements were performed in the scattering-limited regime, by fabricating SiO<sub>2</sub> toroid micro-cavities doped with Si NCs. Si NCs exhibit quantum-confined photoluminescence (PL) in the visible and near-infrared, and have various potential applications in photonic and electronic devices[8]. Si NCs do not possess significant absorption transitions at  $\lambda = 1.5 \mu\text{m}$  and have a high refractive index relative to the SiO<sub>2</sub> matrix ( $n = 3.48$  vs.  $n = 1.44$ ) and thus act (in the 1550-nm band) as strong scattering centers. The Si NC doped cavities were made by ion-implantation of 900 keV Si<sup>+</sup> ions (fluence  $9.1 \times 10^{16} \text{ cm}^{-2}$ ) into a thermally oxidized Si wafer (2  $\mu\text{m}$  oxide),

followed by annealing[9] and toroid fabrication. In order to confirm the presence of Si NCs after fabrication, 2-D cross-sectional PL images were measured using a confocal imaging microscope (using a rhodamine doped index matching oil). Figure 2(a) shows a cross sectional image of the integrated PL in the 650 – 690 nm band, taken in the toroid’s equatorial plane. A bright luminescent ring is observed, characteristic of quantum-confined emission from Si NCs embedded in the toroid. The emission spectrum (cf. Fig.2) peaks at  $\lambda = 675$  nm, corresponding to a NC diameter of  $\sim 3$  nm. A cross sectional image of the toroid’s minor ring is shown in Fig. 2 ( resolution of  $400 \times 850$  nm). Clear NC PL is again observed inside the toroidal ring. The outer PL ring in Fig. 2 corresponds to emission from the rhodamine dye adsorbed onto the surface, and serves to determine the cavities’ outer contour. We find that while the NC PL is inhomogeneously distributed, Si NC PL is observed throughout the entire toroidal volume.

The optical resonances of Si NC doped microcavities exhibited splitting frequencies as large as 1 GHz, nearly two orders of magnitude larger than for the undoped SiO<sub>2</sub> toroids. This confirms that scattering centers (here Si NCs) are responsible for the observed strong modal coupling (i.e.  $\Gamma \gg 1$ ). The highest observed modal coupling parameter was  $\Gamma = 50$ . Correspondingly, according to Eq. 5, the capture efficiency is  $\eta > 98\%$ . Thus despite strong scattering from the NCs, long photon storage times are still achievable. Indeed, Q-factors  $> 10^7$  are observed for most measured resonances.

In order to obtain an even more exact value of the capture efficiency, two different sets of transverse cavity modes (attributed to the radial mode index  $n = 1$  and  $n = 2$ ) were characterized with progressing angular mode numbers ( $\ell, \ell + 1, \ell + 2, \dots$ ). Due to the inhomogeneous distribution of the NCs (cf. Fig. 2), these modes are dominated by differing levels of scattering. However, due to the presence of water and OH adsorbed onto the cavity surface, each set of radial modes experiences the same amount of residual absorption.  $\Gamma$  and  $Q$  measurements for each of these resonances are shown in Fig. 3 where the splitting frequency is expressed as splitting quality factor  $Q_{split} = \omega\gamma$ . The solid line in Fig. 3 is a two-parameter ( $\eta$  and  $\tau_0$ ) fit of Eq. 3 applied to the high-Q experimental data (attributed to the  $n = 1$  radial modes), and excellent agreement is obtained for  $\eta = 99.42\%$  ( $\pm 0.04\%$ ) and  $\tau_0 = 115$  ns ( $\pm 3$  ns) (i.e.  $Q_0 = 1.4 \times 10^8$ ). The deviation between fit and data for the lower-Q data is attributed to higher-order radial modes ( $n = 2$ ), which possess increased intrinsic (OH and water) absorption losses, owing to their slower decaying field amplitude

outside the cavity. The mode identification is also consistent with the inhomogeneous distribution of NCs, which causes increased scattering for higher order radial modes (cf. Fig. 2). These modes follow absorption-limited Q behavior, represented by a constant  $Q_{scat}$ , (and a linear dependence of  $\Gamma(Q)$ , see inset Fig. 3). The inferred intrinsic cavity lifetime  $\tau_0$  is in good quantitative agreement with recent estimates of the absorption loss due to water adsorbed onto the cavity surface.[7] The remarkably high capture efficiency of 99.42% found here clearly demonstrates that optical scattering in microcavities occurs preferentially into cavity eigenmodes.

This observation can be understood by the following qualitative reasoning. For a single nanoparticle coupled to a microcavity mode, the temporal confinement of light implies periodic scattering with the temporal periodicity given by the cavity round-trip time. Conversely, one can treat the problem as scattering by a chain of  $M$  equidistantly spaced scattering centers (spatial periodicity of  $L = 2\pi R$ ). The incident optical field will induce a dipole moment  $\vec{p}$ , which is in phase at each scattering site. The number ( $M$ ) of excited dipoles is approximately given by the cavity lifetime divided by the round trip time ( $T$ ) i.e.

$$M \simeq \frac{\tau c}{2\pi n_{eff} R} = \frac{Q\lambda}{4\pi^2 R n_{eff}} \quad (6)$$

This problem can be recognized as 1-D scattering of a periodic lattice and is well known in solid state physics or diffractive optics. The interference of all  $M$  scattering centers, leads to a scattering intensity (i.e. diffraction pattern) with a width of the corresponding principal diffraction maxima as given by:  $\Delta\theta = \frac{2\pi}{M}$ . Therefore, the on-axis scattering rate is enhanced by the cavity by a factor of  $M$ , compared to the peak scattering rate of a single emitter (dipole) in free space i.e.  $\left(\frac{dP}{d\Omega}\right)_{\theta=0}^{(M)} = M \left(\frac{dP}{d\Omega}\right)_{\theta=0}^{(single)}$ . This angular narrowing of the spatial emission profile due to a collection of dipoles has been treated in the context of super-radiance[10] and pertains both to an atomic (quantum) dipole as well as to a classical system of radiators. Note that  $M$  is proportional to  $Q/V_m$  where  $V_m$  is the mode volume. This motivates a second interpretation, by considering the effect of DOS in the scattering process.

If we consider  $\vec{E}_d$  to be the dipole field, then the probability of scattering into a designated plane wave with wave vector  $\vec{k}$  and polarization  $\vec{\sigma}$  is proportional to the integral  $\epsilon \int \vec{E}_{k,\sigma} \cdot \vec{E}_d dV$ . [11] The total scattering rate is obtained by summation over all possible modes. Correspondingly, if the DOS is altered – e.g. due to the presence of a cavity – the

emission into certain modes is enhanced, while emission into others is suppressed. The enhancement of scattering is therefore given by the ratio of the optical DOS in the microcavity to the value of free space, which at resonance is given by[12]

$$F = \frac{3}{4\pi^2} \frac{Q}{V} \left( \frac{\lambda}{n} \right)^3 \quad (7)$$

i.e. the well known *Purcell factor*. An explicit mathematical derivation of the enhancement as outlined here has also been undertaken and will be communicated elsewhere.

Note that an excited atom within a high-Q microcavity (in the regime of weak coupling), will also preferentially emit into the cavity mode. This is referred to as the Purcell *effect*, and the corresponding shortening of the spontaneous emission (SE) lifetime is given by the Purcell factor as first proposed in Ref. [12]. Note that the origin of preferential emission for an atomic and a classical dipole are identical; for an atom the enhancement of SE follows from classical electrodynamics, and results from the enhanced DOS of the vacuum field[13]. Furthermore, atomic SE enhancement can be interpreted in terms of a chain of radiating dipoles (as done here in the case of scattering) when using the image method, which replaces the cavity mirrors (in case of a Fabry- Pérot cavity) by an infinite chain of image dipoles[14].

Having established the relation of preferential scattering and the optical density of states, we can now relate the capture efficiency  $\eta$  to the Purcell factor via:

$$\eta = \frac{F}{F + 1} \quad (8)$$

as in the case of an atomic emitter ( $\beta$  factor). The experimentally found value of  $\eta = 99.42 \pm 0.04\%$  (cf. Fig. 3) then corresponds to a Purcell factor  $F = 172 \pm 10$ . This represents the highest measured value of this parameter to date. Theoretically, the Purcell factor for the toroid microcavities used in the experiments ( $Q = 1.3 \times 10^8$ ,  $D = 72\mu m$ ,  $A_{eff} = 14\mu m^2$ ) equals  $F = 2060$ , corresponding to  $\eta = 99.95\%$ . The discrepancy between this and the experimentally found value is likely to be caused by the presence of minute absorption (originating from defect-related mid-gap states, or from two-photon absorption in the Si NCs). Taking absorption into account, the modal coupling parameter is given by:

$$\Gamma = \left( \frac{\frac{1}{2}\eta\gamma_{tot}^{-1}}{\tau_0^{-1} + (1 - \eta)\gamma_{tot}^{-1} + \frac{\sigma_{abs}}{\sigma_{scat}}\gamma_{tot}^{-1}} \right) \quad (9)$$

with  $\sigma_{abs}$  being the absorption cross section. Repeating the fit of data in Fig 3. with Eqs. 9 we obtain,  $\tau_0^{-1} = 115 \pm 3.5 \text{ ns}$ ,  $\left( \frac{\sigma_{abs}}{\sigma_{scat}} \right)^{-1} = 211 \pm 15$  and  $\eta = 99.89 \pm 0.04\%$ . The

equivalent Purcell factor is  $F = 883 (+484/ - 229)$  and is in better agreement with the theoretical prediction. The remaining discrepancy is attributed to the fact that scattering centers located at different positions in the toroid experience the *local* density of states, which is lower than the value given by eqs. 7. Therefore the measured value corresponds to the local D.O.S averaged over the spatial distribution of the scattering centers.

In conclusion, we have analyzed and determined for the first time the capture efficiency of scattered light in an optical micro-cavity. For a toroidal microcavity doped with silicon nanocrystals, 99.89% of the scattered light is preferentially scattered into a cavity mode, equivalent to a more than two order of magnitude increase of the scattering rate into the microcavity mode with respect to the free space scattering rate. This enhancement is found to be related to the ratio of the optical density of states in the microcavity to that of free space, as given by the Purcell-factor, and is an intrinsic property of any microcavity. Equally important, our results demonstrate that the Purcell factor of an whispering-gallery mode microcavity can be measured directly via the observed modal coupling.

#### A. Acknowledgements

We thank Prof. S. Roorda (Université de Montréal) for Si ion implantation. This work was funded by the DARPA, the NSF, and the Caltech Lee Center. The Dutch part of this work is part of the research program of FOM, which is financially supported by NWO. A.T. is grateful to the Fonds NATEQ (Québec, Canada) for a postdoctoral scholarship. T.J.K. acknowledges a postdoctoral scholarship from the IST-CPI. The authors acknowledge Dr. Oskar Painter for valuable discussions.

- 
- [1] K. J. Vahala, Nature **424**, 839 (2003).
  - [2] M. L. Gorodetsky, A. D. Pryamikov, and V. S. Ilchenko, Journal of the Optical Society of America B-Optical Physics **17**, 1051 (2000).
  - [3] D. S. Weiss, V. Sandoghdar, J. Hare, V. Lefevreseguin, J. M. Raimond, and S. Haroche, Optics Letters **20**, 1835 (1995).
  - [4] T. J. Kippenberg, S. M. Spillane, and K. J. Vahala, Optics Letters **27**, 1669 (2002).

- [5] D. K. Armani, T. J. Kippenberg, S. M. Spillane, and K. J. Vahala, *Nature* **421**, 925 (2003).
- [6] S. M. Spillane, T. J. Kippenberg, O. J. Painter, and K. J. Vahala, *Physical Review Letters* **91**, art. no. (2003).
- [7] H. Rokhsari and K. J. Vahala, *Applied Physics Letters* **85**, 3029 (2004).
- [8] A. Polman, *Nature Materials* **1**, 10 (2002).
- [9] K. S. Min, K. V. Shcheglov, C. M. Yang, H. A. Atwater, M. L. Brongersma, and A. Polman, *Applied Physics Letters* **69**, 2033 (1996).
- [10] N. Rehler and J. Eberly, *Physical Review A* **3**, 1735 (1971).
- [11] K. J. Vahala, *Pure Appl. Opt.* **2**, 549 (1993).
- [12] E. M. Purcell, *Phys. Rev.* **69** (1946).
- [13] P. Milonni, *The Quantum Vacuum* (Academic Press, 1994).
- [14] P. Milonni and P. Knight, *Optics Communication* **9**, 119 (1973).

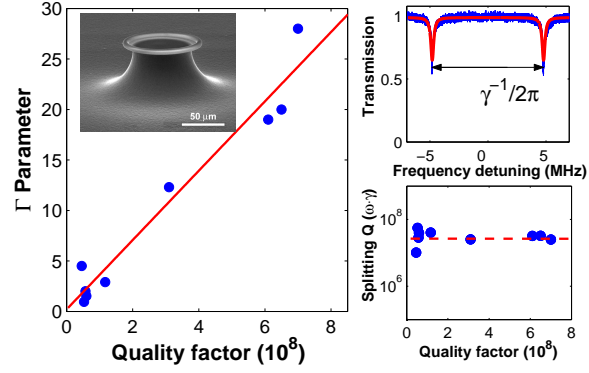


FIG. 1: Left figure: Modal coupling parameter (or doublet “visibility”)  $\Gamma$  as a function of  $Q$  for several fundamental modes of a  $\text{SiO}_2$  toroid microcavity. A SEM micrograph of a toroid microcavity is shown as inset. Upper right: characteristic spectral scan, showing a typical mode splitting of  $\sim 10$  MHz and  $\Gamma \sim 30$ . Lower right panel: Splitting  $Q_{split} (= \omega\gamma)$  as a function of  $Q$ , which is nearly identical for all modes of the resonator.

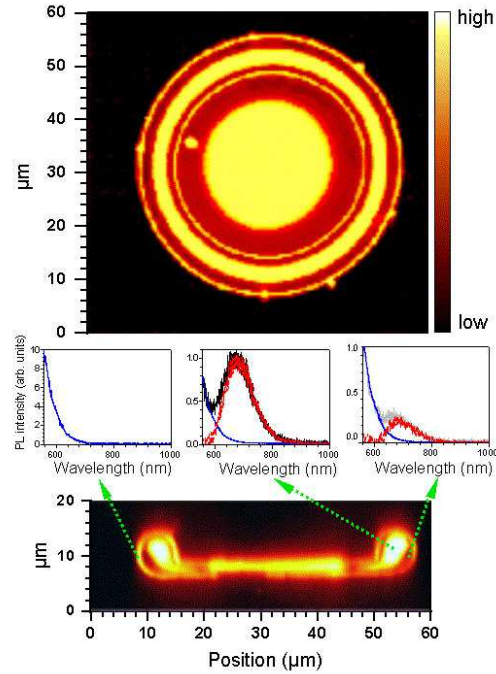


FIG. 2: Cross-sectional confocal PL images taken on a  $72\text{-}\mu\text{m}$ -diameter Si NC doped  $\text{SiO}_2$  toroidal microcavity. Photoluminescence is collected in 650-690 nm band. (a) x-y cross section. (b) y-z cross section. Both images are taken with the toroid immersed into index-matching oil doped with rhodamine. The insets show PL spectra taken at characteristic locations in the toroid. The outer bright line in both images is attributed to the PL of the rhodamine dye and serves to determine the cavity's outer contour.

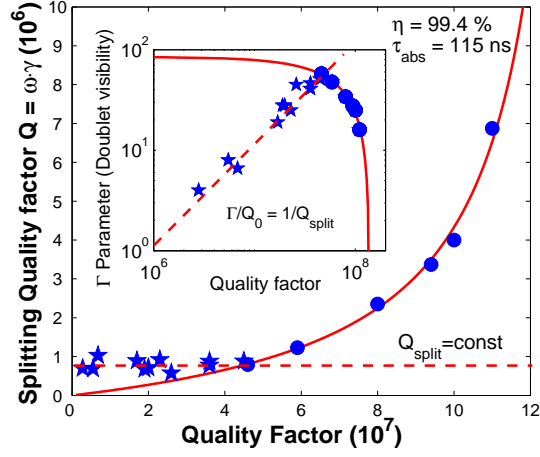


FIG. 3: Splitting quality factor ( $Q_{split} = \omega\gamma$ ) as a function of  $Q$  for the microcavity from Fig. 2. Inset: Same data, plotted as  $\Gamma$  as a function of  $Q$ . The solid line in both graphs is a two-parameter fit using Eq. (3) to the scattering-limited WGMs (closed circles), yielding  $\tau_0 = 115.2 \pm 3$  ns, and  $\eta = 99.42 \pm 0.04\%$ . The low- $Q$  data (stars), fitted with the dashed lines, correspond to higher-order (absorption limited) radial modes (Eq. (4))